Supplemental methods

Table of contents

1 Computational methods

Model description

The principal scheme of the circadian clock is shown in Figure 1 of the Results. A more detailed scheme in SBGN notation (http://www.sbgn.org) is presented in Supplementary Figure 1. The model that corresponds to this scheme is described by the system of ordinary differential equations (ODEs):

$$\frac{dc_L^m}{dt} = \frac{{g_1}^a}{{g_1}^a + (c_{P9} + c_{P7} + c_{NI})^a}(L \cdot q_1 \cdot c_P + n_0 L + n_1 \cdot \frac{{c_{T\,\mathrm{mod}}}^b}{{c_{T\,\mathrm{mod}}}^b + {g_2}^b}) - (m_1 L + m_2 D) \cdot c_L^m \quad (1)$$

$$\frac{dc_L}{dt} = (p_1 L + p_2 D) \cdot c_L^m - m_3 c_L - p_3 \frac{{c_L}^c}{{c_L}^c + {g_3}^c} \quad (2)$$

$$\frac{dc_{L\,\mathrm{mod}}}{dt} = p_3 \frac{{c_L}^c}{{c_L}^c + {g_3}^c} - m_4 c_{Lm} \quad (3)$$

$$\frac{dc_T^m}{dt} = (n_2 \frac{{c_Y}^d}{{c_Y}^d + {g_4}^d} + n_3) \cdot \frac{{g_5}^e}{{g_5}^e + {c_L}^e} - m_5 c_T^m \quad (4)$$

$$\frac{dc_T}{dt} = p_4 c_T^m - (m_6 L + m_7 D) \cdot c_T (c_{ZTL} \cdot p_5 + c_{ZG}) - m_8 c_T \quad (5)$$

$$\frac{dc_{T\,\mathrm{mod}}}{dt} = p_{15} \frac{{c_T}^f}{{c_T}^f + {g_6}^f} - (m_{25} L + m_{26} D) \cdot c_{Tm} \quad (6)$$

$$\frac{dc_Y^m}{dt} = L q_2 c_P + (n_5 L + n_6 D) \cdot \frac{{g_7}^s}{{g_7}^s + {c_T}^s} \frac{{g_{16}}^g}{{g_{16}}^g + {c_L}^g} - m_9 c_Y^m \quad (7)$$

$$\frac{dc_Y}{dt} = p_6 c_Y^m - m_{10} c_Y \quad (8)$$

$$\frac{dc_P}{dt} = p_7 D \cdot (1 - c_P) - m_{11} c_P L \quad (9)$$

$$\frac{dc_{P9}^m}{dt} = L \cdot q_3 \cdot c_P + n_7 \cdot \frac{{g_8}^h}{{g_8}^h + {c_T}^h} \cdot \frac{{c_L}^i}{{g_9}^i + {c_L}^i} - m_{12} c_{P9}^m \quad (10)$$

$$\frac{dc_{P9}}{dt} = p_8 c_{P9}^m - (m_{13} L + m_{22} D) \cdot c_{P9} \quad (11)$$

$$\frac{dc_{P7}^m}{dt} = n_8 \frac{{c_{Ltot}}^j}{{g_{10}}^j + {c_{Ltot}}^j} + n_9 \frac{{c_{P9}}^k}{{g_{11}}^k + {c_{P9}}^k} - m_{14} c_{P7}^m \quad (12)$$

$$\frac{dc_{P7}}{dt} = p_9 c_{P7}^m - (m_{15} L + m_{23} D) \cdot c_{P7} \quad (13)$$

$$\frac{dc_{NI}^m}{dt} = n_{10} \frac{{c_{L\,\mathrm{mod}}}^l}{{g_{12}}^l + {c_{L\,\mathrm{mod}}}^l} + n_{11} \frac{{c_{P7}}^m}{{g_{13}}^m + {c_{P7}}^m} - m_{16} c_{NI}^m \quad (15)$$

$$\frac{dc_{NI}}{dt} = p_{10} c_{NI}^m - (m_{17} L + m_{24} D) \cdot c_{NI} \quad (15)$$

$$\frac{dc_G^m}{dt} = L \cdot q_4 \cdot c_P + \frac{{g_{14}}^n}{{g_{14}}^n + {c_T}^n} \cdot \frac{{g_{15}}^o}{{c_L}^o + {g_{15}}^o} \cdot n_{12} L - m_{18} c_G^m \quad (16)$$

$$\frac{dc_G}{dt} = p_{11} c_G^m - p_{12} L c_{ZTL} c_G + p_{13} c_{ZG} D - m_{19} c_G \quad (17)$$

$$\frac{dc_{ZTL}}{dt} = p_{14} - p_{12} L c_{ZTL} c_G + p_{13} c_{ZG} D - m_{20} c_{ZTL} \quad (18)$$

$$\frac{dc_{ZG}}{dt} = p_{12} L c_{ZTL} c_G - p_{13} c_{ZG} D - m_{21} c_{ZG} \quad (19)$$

Where c_i^m and c_i stand for dimensionless concentrations of mRNA and protein, respectively, which reach a maximum level of 1 in wild-type (wt) plants in 12L:12D conditions. The time unit is an hour. Index "*i*" labels the molecular components

LHY/CCA1 mRNA or protein (L), LHY/CCA1 modified protein (Lmod), total amount of LHY/CCA1 protein (Ltot), TOC1 mRNA or protein (T), TOC1 modified protein $TOC1_{mod}$ (Tmod), mRNA and proteins for Y (Y), PRR9 (P9), PRR7 (P7), NI (NI), GI (G); ZTL protein (ZTL), ZTL-GI protein complex (ZG). The parameters n_j, m_j represent the rate constants of transcription and degradation, respectively; p_j are constants of translation, protein modification and protein complex formation; g_j are Michaelis-Menten constants and *a, b, c, d, e, f, g, h, i, j, k, l, m, n, o, s* are Hill coefficients; q_j are the rate constants of acute (P-dependent) light activation of transcription. The acute light response in activation of *PRR9, LHY/CCA1, GI, Y* transcription was modeled analogous to (Locke et al, 2006) using a light-sensitive activator – protein P (c_P), which is accumulated in darkness and was degraded in light. L=1 when light is present, 0 otherwise; D=1-L. The $\theta(t)$ function was used to simulate the smooth transitions between L and D analogous to (Akman et al, 2008):

$$L(t) = \theta(t) = 0.5 \cdot ((1 + \tanh((t - 24 \cdot floor(t/24) - dawn)/T)) - (1 + \tanh((t - 24 \cdot floor(t/24) - dusk)/T)) + (1 + \tanh((t - 24 \cdot floor(t/24) - 24)/T)))$$

Where *dawn* and *dusk* are the phases of dawn and dusk (normally *dawn=0*); T is the duration of twilight (we used T=0.5 h); tanh and floor – standard functions of hyperbolic tangent and rounding operation.

Mutations of the clock genes except ZTL were simulated by setting the rate of the genes transcription to zero (unless described otherwise in the text). Mutation of ZTL was simulated by setting the ZTL translation rate to zero.

The mathematical description of the scheme was simplified compared to the previous model (Locke et al, 2006) by reducing the number of intermediate species of the same substance (one variable for mRNA and only one for protein, except LHY/CCA1 and TOC1 proteins). The degradation of all species was described by first order kinetics, which corresponds to biological systems with a high capacity of the degradation system.

The equations were solved using MATLAB, integrated with the stiff solver ode15s (The MathWorks UK, Cambridge). SBML versions of the model will be available from the Molecular Systems Biology website (www.nature.com/msb), the Biomodels database (Le Novere et al, 2006) (accession number MODEL1007240000) and the

Plant Systems Modelling repository (www.plasmo.ed.ac.uk). MATLAB versions of the model are available from the corresponding author upon request. CVODE software was used for the parameter stability analysis (Hindmarsh AC, 2005).

Parameter values were either constrained based on experimental data (see description below and Supplementary Table 1), or fitted to multiple timeseries data sets. In total, 35 parameters were constrained and 55 parameters were fitted. The fitting procedure minimized the deviation of simulated mRNA profiles from experimental data on wt plants, entrained in 12L:12D cycles, for the following genes: *LHY* and *CCA1* (Farre et al, 2005), (Edwards K. et. al., in preparation), *PRR9* and *PRR7* (Nakamichi et al, 2003), *GI* (Kim et al, 2007; Locke et al, 2005), *TOC1* (Nakamichi et al, 2005). We also fitted the values of free running periods of wt plants in constant light (LL) and constant dark (DD) conditions and periods of *lhy/cca1*, *toc1*, *ztl* and *prr7/prr9* mutants in LL conditions. The optimal parameter values are shown in Supplementary Table 1. The period values for the optimal parameters were 24.7 h for wt in LL; 27.6 h for wt in DD; and 17.3 h, 21 h, 28.3 h, 27.5 h for *lhy/cca1*, *toc1*, *ztl* and *prr7/prr9* mutants in LL, which correspond to experimental data (Farre et al, 2005; Locke et al, 2005; Mas et al, 2003a; Mas et al, 2003b; Millar et al, 1995; Strayer et al, 2000). Additionally, the parameter values were chosen such that the mRNA levels of all gene expression peaked at a level of 1 for wt plants in 12L:12D condition.

The extended clock circuit

The model assumptions, which were based either on direct or indirect experimental observations are summarized below.

1) *LHY/CCA1* transcription was described analogous to our previous model (Locke et al, 2006), hereafter referred as L2006. Transcription is assumed to be activated by light through an acute light response mediated by protein P and a P-independent light activation. Additionally it was assumed to be activated by activator $TOC1_{mod}$. *LHY/CCA1* transcription is inhibited by inhibitors PRR9, PRR7 and "night" inhibitor (NI), which in part represents PRR5. The acceleration of *LHY/CCA1* mRNA degradation in the light compare to darkness (parameter $m_1>m_2$) was based on the data (Yakir et al,

2007) consistent with our experimental measurements of *CCA1* mRNA stability (Supplementary Figure 18).

2) The activation of LHY/CCA1 translation by light ($p_1>p_2$) and post-translational modification of LHY/CCA1 were introduced based on (Daniel et al, 2004; Kim et al, 2003). Post-translational modifications of LHY and CCA1 and the formation of multi-protein complexes are represented by the modified form of LHY/CCA1 protein (LHY_{mod}), which accumulates later in the day than the unmodified protein.
3) *TOC1* transcription was described analogous to L2006 by assuming its activation by Y and inhibition by LHY/CCA1. Additionally we included Y-independent basal activation of *TOC1* transcription based on the observed high background expression of *TOC1* at the end of the night (Nakamichi et al, 2003).
4) The kinetics of TOC1 protein was described through its translation and targeted degradation by ZTL (Kim et al, 2007), which is accelerated in darkness ($m_7>m_6$) (Mas et al, 2003b). Both free and GI-bound ZTL is assumed to be active in TOC1 degradation. We also assumed ZTL-independent degradation of TOC1 protein based on the data of its degradation through other F-box proteins (Baudry et al, 2010)
5) We replace the X component from L2006 by $TOC1_{mod}$, which represents an activating complex at LHY/CCA1 promoter. It was assumed that the formation of this complex can be related to post-translational modification of TOC1, although the complex may also include some other night components (Pruneda-Paz et al, 2009). As the details of $TOC1_{mod}$ formation are yet unknown, we assumed that $TOC1_{mod}$ is more stable in darkness than in light ($m_{25}>m_{26}$) in order to describe the experimentally observed delay between *TOC1* expression at dusk and the activation of *LHY/CCA1* expression around dawn.
6) The transcription of *Y* is described similarly to L2006 and includes its acute activation by light through protein P and by P-independent light activation ($n_5>n_6$) as well as the inhibition by TOC1 and LHY proteins.
7) Protein P is described analogous to L2006 through its accumulation in dark and degradation in light. Protein P represents a photoreceptor-related

transcription factor, which participates in the acute light transcription of *LHY/CCA1*, *PRR9*, *GI* and *Y* after dawn.

8) The inhibitors PRR9, PRR7, NI were assumed to be transcribed sequentially based on (Nakamichi et al, 2003). The transcription of *PRR9* and *PRR7* is known to be activated by LHY/CCA1 (Farre et al, 2005), but the actual mechanism, which ensures the time delays in each inhibitor after another is unknown. To describe the wave of inhibitor we assumed that they activate each other (*PRR7* by PRR9 and *NI* by PRR7) and they are also activated differently by different forms of LHY: *PRR9* is activated by LHY protein, *NI* by LHY_{mod}, and *PRR7* by both LHY and LHY_{mod}. Additionally, the experimentally observed acute activation of *PRR9* expression by light and inhibition of *PRR9* expression by TOC1 was included into the equation for *PRR9* mRNA (Makino et al, 2002).
9) Based on experimental observations (Farre & Kay, 2007; Ito et al, 2007; Kiba et al, 2007), we included the accelerated degradation of PRR9, PRR7 (and by extension, NI) proteins in darkness compare to light ($m_{22}>m_{13}$; $m_{23}>m_{15}$; $m_{24}>m_{17}$).
10) *GI* transcription was described analogous to *Y*, with acute P-dependent and P-independent light activation , and inhibition by TOC1 and LHY proteins. The stabilization of ZTL protein through its binding to GI protein in presence of light and the dissociation of GI-ZTL complex in the dark were based on the experimental results (Kim et al, 2007). GI protein does not participate in *TOC1* gene regulation (Martin-Tryon 2007), in contrast to L2006.
11) ZTL translation rate was assumed to be constant based on data on uniform *ZTL* mRNA expression (Kim et al, 2007).

The more detailed description of the model properties and the comparison of the model to L2006 is presented below.

In L2006 LHY/CCA1 transcription was activated by light and activator X and inhibited by one inhibitor PRR9/7. In our model the activator X was replaced with $TOC1_{mod}$ and there are three inhibitors PRR9, PRR7 and NI. In addition to the “day” inhibitors PRR9 and PRR7, we included a “night” inhibitor (NI) to account for the very low expression of *LHY/CCA1* at the beginning of the night. Supplementary Figure 2 below shows experimental profiles of *LHY* and *CCA1* mRNA, which

demonstrate strong repression of *LHY* and *CCA1* by the circadian clock (note the log scale).

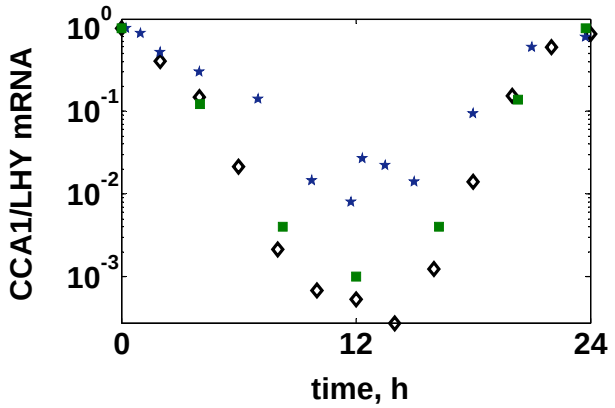

Supplementary Figure 2. Robust regulation of *CCA1* and *LHY* mRNA level by the circadian clock in wt plants during 12L:12D entrainment. Experimental data on *CCA1* and *LHY* expression show a very low level of mRNA in the early night. Different symbols correspond to different sets of data: *LHY* mRNA - square (Farre et al, 2005), *CCA1* mRNA - diamonds (Edwards K. et. al., in preparation) and pentagram (Southern, 2005).

Both activator and inhibitors of *LHY/CCA1* are regulated by the total duration of light in the current model, *via* light-regulated protein degradation, whereas the only light induction of *PRR9/7* occurred transiently in the morning (P-dependent) in L2006. This additional regulation of *LHY/CCA1* expression by light in the current model results in the decrease of the peak level of *LHY/CCA1* with the increase of photoperiod length, which agrees with our experimental data (Figure 7 of the Results). Supplementary Figure 3 illustrates this result in more detail by showing the simulated profiles of *LHY/CCA1* mRNA and PRR9, PRR7, NI, $TOC1_{mod}$ proteins for short (6L:18D) and long (18L:6D) days. The model predicts that the accelerated degradation of inhibitor proteins PRR9, PRR7 and NI in darkness compared to light (Farre & Kay, 2007; Ito et al, 2007; Kiba et al, 2007) results in the early rise of *LHY/CCA1* mRNA before dawn in SD. Additionally to the inhibitors, the activator $TOC1_{mod}$ slightly increases the amplitude of *LHY/CCA1* mRNA under short photoperiods, because of the higher stability of $TOC1_{mod}$ in darkness compared to light (*TOC1* mRNA and protein profiles are shown in Supplementary Figure 11).

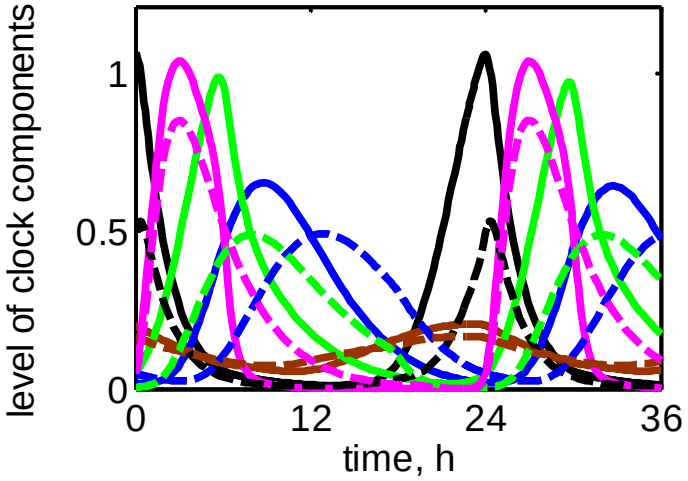

Supplementary Figure 3. Regulation of *LHY/CCA1* phase under various photoperiods in wt plants. Simulated profiles of *LHY/CCA1* mRNA (black) and PRR9 (magenta), PRR7 (green), NI (blue) and $TOC1_{mod}$ (brown) proteins are shown for 6L:18D (solid lines) and 18L:6D (dashed lines). Lights-on occurs at 0h and 24h.

In contrast, L2006 failed to describe our data on *CCA1* expression under various photoperiods (Figure 7 of the Results), as shown on Supplementary Figure 4 below. The *LHY/CCA1* mRNA profile was not sensitive to photoperiod because the photoperiod had negligible effect on its activator X and its inhibitor PRR9/7 in L2006.

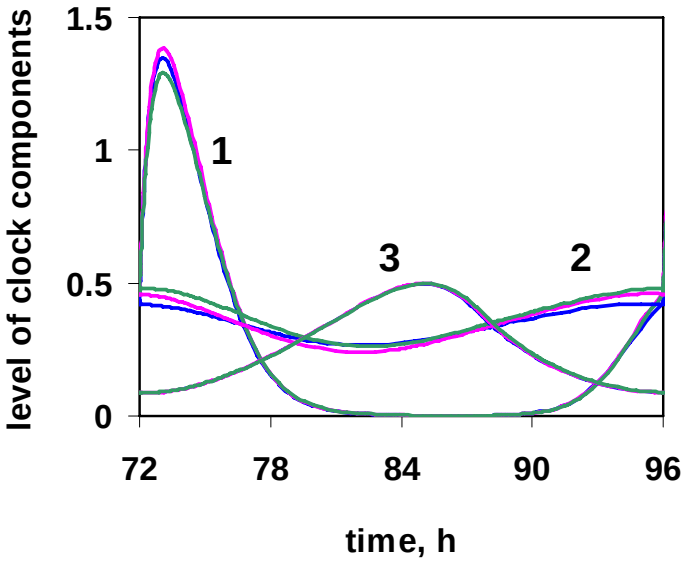

Supplementary Figure 4. Independence of *LHY/CCA1* mRNA profile on the photoperiod in the L2006 model. Simulated profiles of *LHY/CCA1* mRNA (1), X nuclear protein (2) and PRR9/7 nuclear protein (3) are shown for 6L:18D, 12L:12D,

18L:6D conditions (blue, magenta and green lines respectively). The nuclear level of PRR9/7 protein is scaled 0.1 times. Lights-on occurs at 72h in all cases.

In L2006 the inhibitors PRR9 and PRR7 were combined into single model component. The necessity to match the low expression of *LHY* and *CCA1* mRNA in the early night required a broad peak of PRR9/7 inhibitor protein around dusk (Supplementary Figure 4 above). The presence of only one inhibitor with a dusk peak constrained the parameters of L2006: *PRR9/7* transcription could not have a strong acute light response, because this would have caused a premature rise in PRR9/7 protein. The weak light activation of *PRR9/7* resulted in weak entrainment of the clock to LD cycles. The model solution reached the entrained limit cycle very slowly, after twenty to one hundred days of entrainment (unpublished results). We also found that L2006 could not describe the "dawn" preference of *CCA1* induction during skeleton entrainment of wt plants (Figure 8B in Results). Rather, the model showed the highest level of *LHY/CCA1* mRNA induction in the "dusk" light pulse (data not shown). The introduction of two inhibitors PRR9 and PRR7 allowed us to avoid these problems by separating the acute light induction of *PRR9* from the inhibition of *LHY/CCA1* in the early night. Strong acute activation of *PRR9* in the current model matches the experimental data and allows fast entrainment of the model to different light conditions. The current model usually reaches its limit cycle within 4 days under various entrainment conditions.

Preliminary simulations of a model variant with only two inhibitors of *LHY/CCA1*, based upon PRR9 and PRR7, showed that the resulting profile of *LHY/CCA1* expression during light-dark cycles had a phase advance and a slower rising phase compared to experimental data. The introduction of the third inhibitor NI resulted in the appropriate delay and sharp rise of *LHY/CCA1* mRNA at night, which matches the data (Figure 6 of the Results).

To investigate the relative importance of PRR7 and NI in the entrainment of the clock to SK in the model, we compared the simulated *prr7* and *ni* single and *prr7/ni* double mutants with wt plants. Supplementary Figure 5B shows that the *prr7/ni* double mutant completely lost the dawn preference of *LHY/CCA1* expression under SK that was observed for wt (Supplementary Figure 5A). The effect was much weaker in

single *ni* and *prr7* mutants (Supplementary Figures 5C, D). These results correspond to our experiments on *prr7*, *prr5* and *prr7/prr5* mutants and wt plants (Figure 8 of the Results). The simulated effect of the *ni* single mutation on *LHY/CCA1* (Supplementary Figure 5C below) was not as strong as observed in the *prr5* mutant (Figure 8G of the Results), but the simulated double mutant reveals the significant contribution from *ni* (Supplementary Figure 5B). The difference in *ni* and *prr5* results from the uncertainties in the parameter values required for NI in the model, prior to its identification with PRR5. The simulated and observed phenotypes of single *prr7* mutants (Supplementary Figures 5D and Figure 8H of the Results) confirm that an inhibitor in addition to PRR7 is present at dusk, which would normally be PRR5. The existence of three inhibitors, PRR9, PRR7 and PRR5, is directly supported by the new results published during revision of this manuscript (Nakamichi et al, 2010).

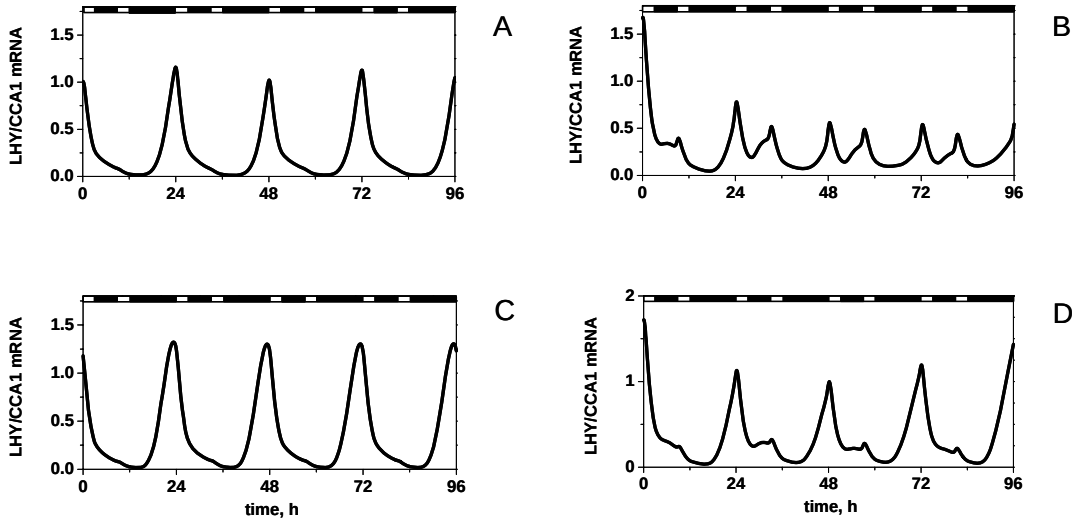

Supplementary Figure 5. The effect of PRR7 and NI on the simulated kinetics of *LHY/CCA1* expression under skeleton photoperiods (SK). The simulations were run under 12L:12D light-dark cycles and then released into the SK entrainment with "dawn" and "dusk" pulses of light, each of 3h duration (3L:6D:3L:12D), at time 0h. The wild type plants (A) and *prr7/ni* (B), *ni* (C), or *prr7* (D) mutants are shown. White and black bars represent the periods of light and dark correspondingly.

To further compare our model with L2006 we analyzed clock entrainment to various T cycles (light/dark cycles of total duration T). Our simulations showed that the L2006 clock model is entrained only in a narrow range of T cycles – between 23 and 26 h (not shown). However the current model can be stably entrained in a wide range

of T, throughout the circadian range from 16h to 36 h. Supplementary Figures 6B, C show the profiles of the clock components under 16 h and 32 h T cycles. Entrainment of the Arabidopsis clock in this range of T was previously described experimentally (Roden et al, 2002). We predict that further increase of T could be supported until the loss of entrainment at T > 48 h. The model allows us to analyze the mechanism of this loss, which is illustrated in Supplementary Figures 6D, E. The increase of T from 24h to 32h leads to an advance of the clock phase (Supplementary Figure 6C), which results in an early fall of $TOC1_{mod}$ at the end of the night. The lower level of the activator decreases *LHY/CCA1* expression levels. Under even longer T cycles, this decrease results in lower levels of PRR9, PRR7, NI at night, allowing a second dawn peak of *LHY/CCA1* expression (Supplementary Figure 6D). The model shows two peaks of LHY/CCA1 per cycle and two inhibitor waves in these conditions, suggesting that it is close to having two internal cycles per entraining cycle. However, further increase of T to 49h results in the loss of entrainment as shown in Supplementary Figure 6E. Thus the inhibitor wave shows some features of an hourglass timer that triggers *LHY/CCA1* expression at a fixed number of hours after dawn. In 24h and shorter T cycles, the hourglass is cut short by rapid degradation of the inhibitor proteins in the dark. The longer T cycles allow the inhibitors to degrade within the light interval, so *LHY/CCA1* expression is initiated irrespective of the subsequent lighting conditions.

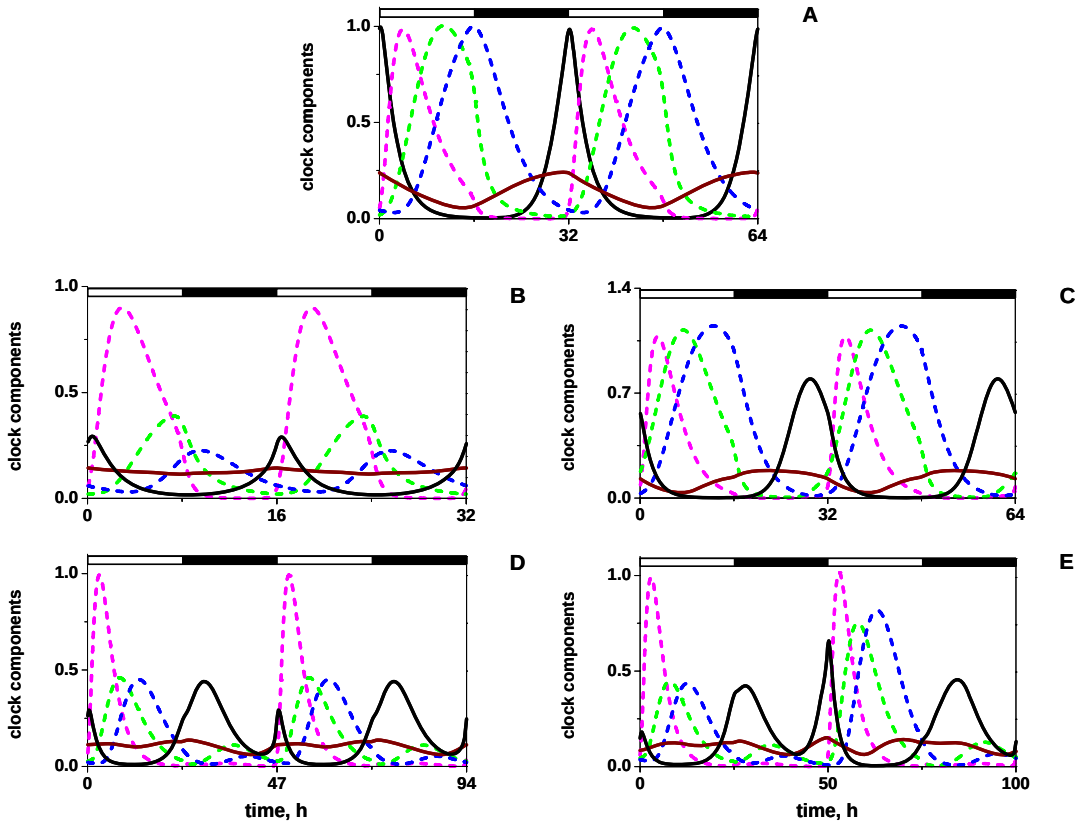

Supplementary Figure 6. Entrainment of the model to various T cycles.
The solutions are shown after they have reached the limit cycle. The duration of T cycles were 24h (A), 16 h (B), 32 h (C), 47 h (D) and 50 h (E). The profiles of *LHY/CCA1* mRNA (black) and PRR9 (magenta), PRR7 (green), NI (blue) and $TOC1_{mod}$ (brown) proteins are shown.

Model simulations showed that the acceleration of LHY/CCA1 translation by light (Kim et al, 2003) allows a strong peak of protein accumulation with the experimentally observed 2-4 hour delay of the protein peak compared to the peak of *CCA1* mRNA. Simulated *LHY* mRNA and protein profiles are shown on Supplementary Figure 7. The model shows good match to the data on *LHY* and *CCA1* mRNA (black) and total LHY protein (blue).

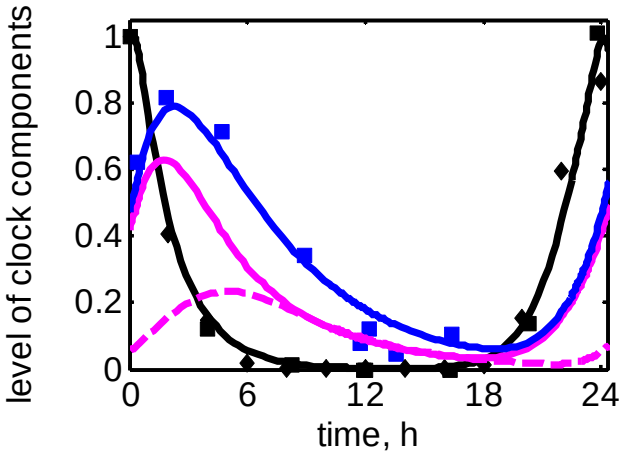

Supplementary Figure 7. Simulated and measured profiles of *LHY/CCA1* mRNA and proteins under 12L:12D conditions in wt plants. Simulated profiles are shown for *LHY/CCA1* mRNA (black line), LHY protein (solid magenta line) and LHY_{mod} (magenta dashed line). The blue line shows the sum of simulated LHY protein and LHY_{mod}. Experimental data for *CCA1* mRNA (black diamonds) are taken from (Edwards K. et. al., in preparation), LHY mRNA (black squares) from (Farre et al, 2005) and for LHY protein (blue squares) from (Kim et al, 2003).

The simulations of the evening component TOC1 showed that the phase of the peak of *TOC1* mRNA expression is determined by both Y and LHY/CCA1 proteins, similarly to L2006. The peak phase therefore showed a similar dependence on photoperiod (Supplementary Figure 8 below), consistent with data (Edwards et al., in preparation).

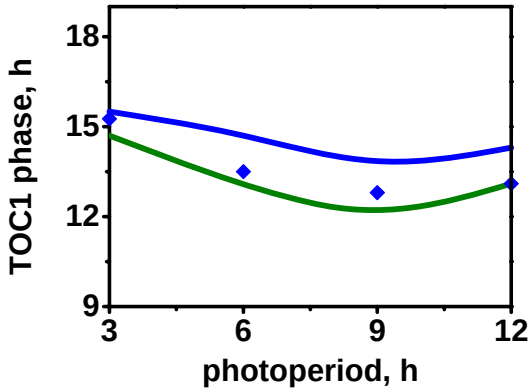

Figure 8. Dependence of the phase of *TOC1* mRNA expression on the day length in wt plants. Simulations are shown by blue and green lines for the current model and

L2006 respectively; experimental data points for *TOC1:LUC* phase are taken from (Edwards K. et. al. in preparation).

The profile of *Y* mRNA expression has two peaks in diurnal conditions, with the first "morning" peak corresponding to the acute light activation of *Y* and the second "dusk" peak resulting from the release of *Y* from its inhibition by LHY/CCA1 (Figure 2A of the Results). However, the profile of *TOC1* mRNA has only a "dusk" peak because the inhibition of *TOC1* transcription by LHY/CCA1 protein suppresses any induction by Y protein in the morning (Figure 2A of the Results). The expression profiles of *Y* and *TOC1* mRNA under light:dark cycles are slightly different for the current and previous models. Supplementary Figure 9 shows the 10-fold higher acute light response of *Y* in L2006 compared to the current model (Figure 2A of the Results).

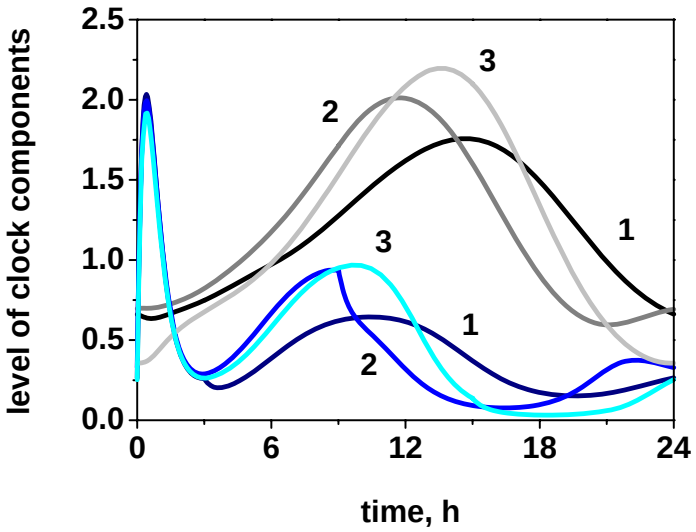

Supplementary Figure 9. Simulated expression profiles of *Y* and *TOC1* in wt plants under different photoperiods for L2006. The profiles of *Y* mRNA are scaled 10 times and shown by dark blue, blue and cyan lines and *TOC1* mRNA by black, grey, light grey lines for 3L:21D (1), 9L:15D (2), 15L:9D (3) respectively.

The difference in the kinetics of the evening loop between the two models becomes especially evident in simulations of the *lhy/cca1* double mutant under different photoperiods. While the *lhy/cca1* mutant in the current model demonstrates considerable changes in the kinetics of *Y* and *TOC1* mRNA expression under different

photoperiods (Figure 2B in the Results), the *lhy/cca1* mutant was completely insensitive to the day length in L2006 (Supplementary Figure 10 below). This was caused by the very slow and substrate-insensitive saturated kinetics of TOC1 protein degradation in L2006, which in turn resulted from a relatively low value of the Michaelis-Menten constant of TOC1 protein degradation. Parameter optimization had thus created a long delay between *TOC1* mRNA and TOC1 protein peaks, which resulted in the loss of dusk sensitivity of *lhy/cca1* mutant (Supplementary Figure 10 below).

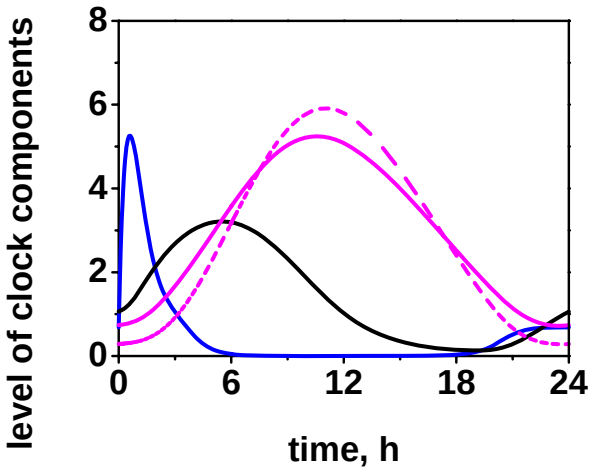

Supplementary Figure 10. Simulated expression profiles of *Y* and TOC1 in the *lhy/cca1* mutant for L2006 under light:dark cycles. The simulation was done under 12L:12D, but the same result was observed under 6L:18D and 18L:6D photoperiods. *Y* mRNA is shown by blue lines, *TOC1* mRNA by black lines and TOC1 protein by magenta lines. *Y* mRNA level scaled 10 times; cytoplasmic and nuclear forms of TOC1 protein are shown by solid and dashed lines respectively. Cytoplasmic level of TOC1 protein scaled 0.1 times.

The absence of sensitivity of *lhy/cca1* mutant to photoperiod in L2006 results from the weak dependence of the rate of TOC1 protein degradation on the concentration of TOC1 protein, which can only be reached in a case of very low level of TOC1 degradation factors relative to TOC1 protein. Although there is no data to refute this assumption, it is natural to assume that the level of regulatory molecules, such as TOC1 protein, should be tightly controlled with an excess of degradation capacity, which is described by the first order kinetics of TOC1 degradation in the current model. Additionally, we included the acceleration of TOC1 protein degradation in

darkness by ZTL. Although the acceleration of TOC1 degradation in darkness was also present in L2006, there was negligible difference between dark and light rates of TOC1 protein degradation under the published parameter values. The above mentioned improvements to our previous model in part of the description of TOC1 protein degradation resulted in the pronounced dependence of *Y* and *TOC1* profiles on photoperiod in lhy/cca1 mutant (Figure 2B of the Results).

The constant of *TOC1* mRNA degradation m5 was measured (Supplementary Figure 18) as described in Experimental Methods section of the Supplementary information. Supplementary Figure 11 below demonstrates the kinetics of the different forms of TOC1 in the model. It shows the time delays between simulated peaks of *TOC1* mRNA (black line), TOC1 protein (magenta line) and $TOC1_{mod}$ (brown line) in wt plants in 12L:12D conditions. The future experiments on the composition of the activator complexes at *LHY* and *CCA1* promoters are necessary to clarify the mechanism of $TOC1_{mod}$ formation and its kinetics.

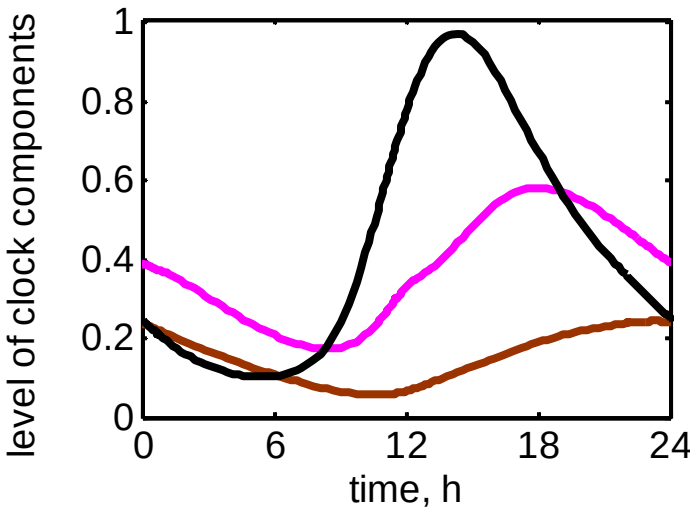

Supplementary Figure 11. Simulated profiles of *TOC1* mRNA and protein in wt plants under 12L:12D conditions. *TOC1* mRNA, TOC1 protein and $TOC1_{mod}$ are shown by black, magenta and brown lines, respectively.

The experimentally observed inhibition of *PRR9* expression by TOC1 was included into the model (Makino et al, 2002). Impairment of this inhibition in the hypothetical partial *toc1* mutant leads to the shortening of the period compared to wt almost to the same extent as in the simulated null *toc1* mutant, as shown on Supplementary Figure

12 below. Analogous to the *toc1* mutant, the elevation of PRR9 level can be related with the observed shortening of the period of *prr9*-overexpressor line (Matsushika et al, 2002).

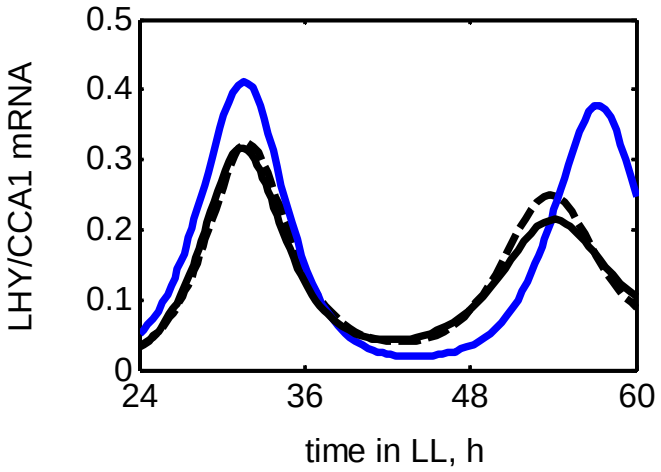

Supplementary Figure 12. Simulated *LHY/CCA1* expression in the partial and null *toc1* mutants under LL conditions. The partial mutant was modeled by removing only the inhibition of *PRR9* expression by TOC1 (shown by dashed black line). The null *toc1* mutant is shown by solid black line. Wild type is shown by blue line for comparison.

The function of GI was separated from Y (see Results). In the current model GI affects the clock through stabilization of ZTL protein in presence of light (Kim et al, 2007). ZTL, in turn, accelerates degradation of TOC1 protein (Kim et al, 2007). In the *gi* mutant, the absence of stabilization of ZTL by GI results in the low level of total ZTL protein (dashed line on the Supplementary Figure 13A below) compared to the total ZTL in wt (solid line), which corresponds to the data (Kim et al, 2007). Next we simulated the kinetics of TOC1 protein in the WT and *gi* mutant, to test whether the model can explain the unexpected experimental observation that TOC1 protein level at night was lower in the *gi* mutant than in WT (Kim et al, 2007). Supplementary Figure 13B shows that TOC1 can indeed be lower in the *gi* mutant than in WT in the later night interval, but TOC 1 is higher in the *gi* mutant than in WT at the beginning of the night, which is related with the lower level of total ZTL in *gi*. Although the TOC1 protein level in WT at the beginning of the night can be increased in the model by decreasing the rate of TOC1 degradation at night by ZTL (parameter m7, blue lines on Supplementary Figure 13B), the difference between TOC1 protein levels in

WT and the *gi* mutant is still less than in the experiment (Kim et al, 2007). The likely explanation relates to differences in ZTL protein function at different phases of the daily cycle. The model made the simple assumption that free ZTL and the GI-ZTL complex were equally active. Experimental results on this and on the interactions of GI and ZTL with other proteins will be required to understand the detailed profiles of TOC1 regulation by GI and ZTL.

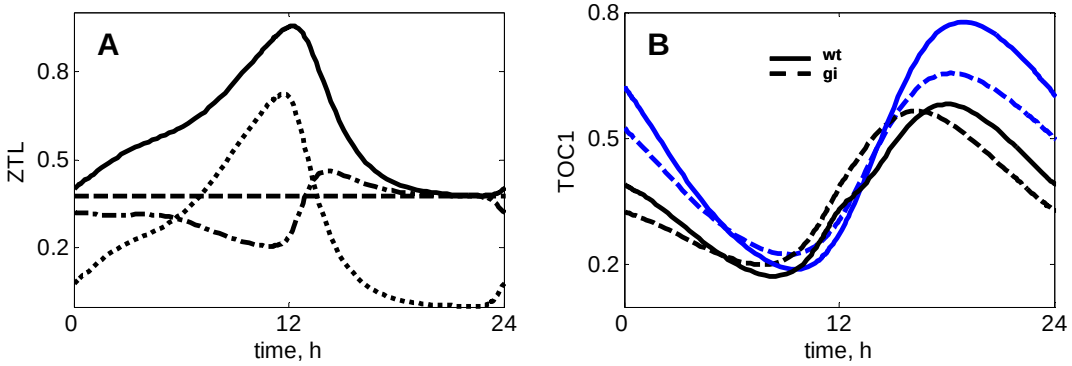

Supplementary Figure 13. Simulated profiles of ZTL and TOC1 proteins during 12L:12D cycle in wt and *gi* mutant plants. A: total ZTL in wt is shown by solid line, ZTL-GI complex in wt – by dot line, free ZTL in wt – by dot-dashed line, free/total ZTL in *gi* mutant is shown by dashed line. B: TOC1 protein in wt is shown by solid line, in *gi* mutant – by dashed line. Black lines correspond to the parameter set, shown in Table 1. Blue lines show simulations with m7=0.25 h^{-1}

The parameters of ZTL translation p_{14} and degradation m_{20} were fitted to multiple timeseries data sets from wt plants and to the period of rhythms in the *lhy/cca1* mutant, as described before. Additional small adjustments of p_{14} and m_{20} were made to improve the description of our skeleton photoperiod data in *prr7/prr5* mutant plants (Figure 8C, D of the Results), when we increased the value of m_{20} 1.2 times (and p_{14} 1.3 times) (the final adjusted values listed in Supplementary Table 1). *GI* mRNA expression was described analogous to L2006. Its activation by light and inhibition by LHY/CCA1 and TOC1 proteins results in a bi-phasic profile of *GI* mRNA (Locke et al, 2005) with small morning and larger afternoon peaks of *GI* expression (analogous to *Y*; Figure 2A of the Results). However, GI protein does not activate *TOC1* transcription directly in the present model.

Parameter stability analysis

The robustness of the model to parameter changes was investigated by measurement of the changes in the period and amplitude of *LHY/CCA1* mRNA in wild type plants in constant light conditions upon 5 % changes of each parameter value. The changes of the period were less than 2 % and amplitude less than 7 %, as shown on Supplementary Figure 14A. This result demonstrates improved robustness of the model compared to L2006, where we had 3% change in the period and 27% change in amplitude (Supplementary Figure 14B).

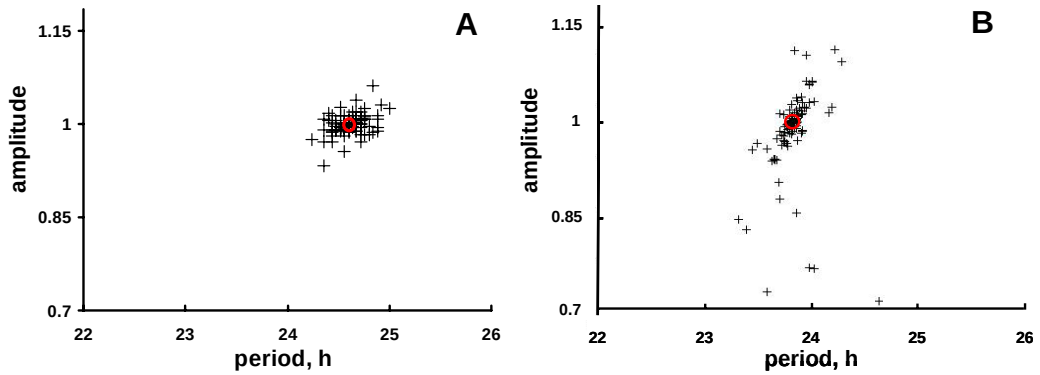

Supplementary Figure 14. Comparison of the robustness of the current (A) and previous (B) models to parameter variations. The relative amplitude and period of *LHY/CCA1* in LL conditions was measured under 5% increase and decrease of each parameter. Panel B is taken from (Locke et al, 2006). The red circles represent the period and amplitude for the optimal parameter values.

We also analyzed the sensitivity of the amplitude and phase of all clock genes in simulations of wt under 12L:12D conditions. The change of clock gene amplitudes was less than 6 % and the phases less than 1.3% upon 5 % changes of parameter values. The individual effects of parameters on the amplitude and phase of different clock genes in 12L:12D are shown in Supplementary Figures 15 and 16.

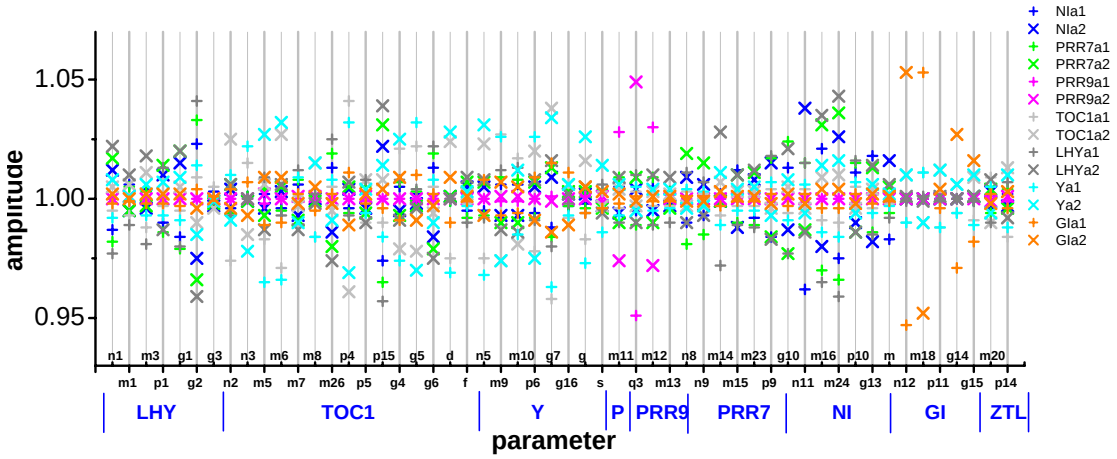

Supplementary Figure 15. Relative changes in the amplitude of clock gene expression in 12L:12D conditions under 5% increase and decrease of each parameter. Only 54 parameters, which are the most sensitive under these conditions are shown. The altered parameters are grouped on the horizontal axis by the gene involved, which are listed under the plot. Plus and cross symbols correspond to the decrease and increase of each parameter, respectively. The clock gene mRNAs that were affected by each parameter change are denoted by the colour of the symbols, as shown in the legend.

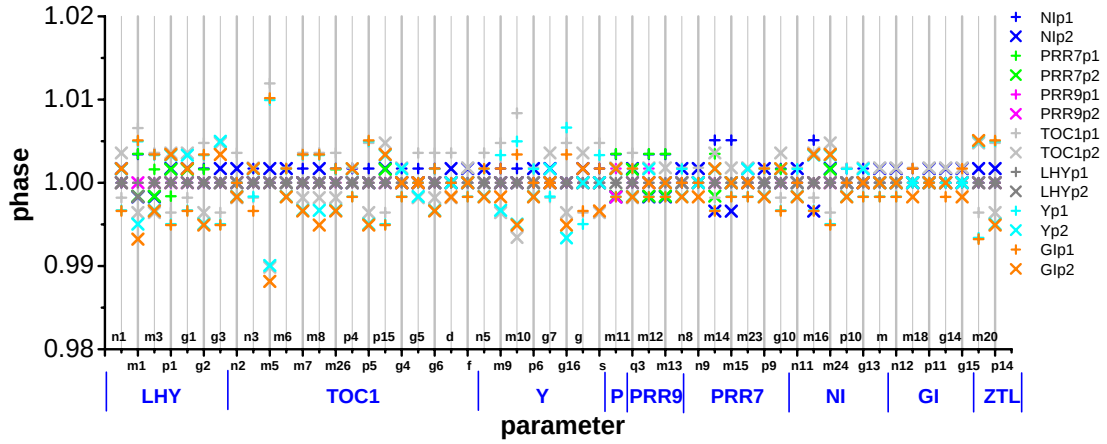

Supplementary Figure 16. Relative changes in the phase of clock gene expression in 12L:12D conditions under 5% increase and decrease of each parameter. Symbols and legend are as in Supplementary Figure 15.

Additionally we measured the sensitivity to parameter variations of the amplitude and period of the simulated wt in LL and DD conditions, and of the period of *lhy/cca1*, *toc1*, *ztl* and *prr7/prr9* mutants in LL. 25 parameters with the most effect on the

properties analyzed were: m_1, m_3, m_5, m_{10}, m_{14}, m_{15}, n_0, n_2, n_7, n_{11}, p_1, p_3, p_4, p_9, p_{15}, g_2, g_3, g_4, g_6, g_7, g_9, g_{10}, g_{13}, a, i. Two of these parameters (m_1, m_5 - *LHY* and *TOC1* mRNA degradation rates) were derived from experimental measurements and two (p_1, m_3 - LHY protein translation and degradation rates) were constrained from the available data. 5 further parameters were constrained based on wt expression profiles under LD cycles, and by the period of the *lhy/cca1* mutant. The 16 remaining parameters were fitted to multiple data types as described above.
The 25 sensitive parameters included processes that affected all components of the model, but only 2 of the 25 sensitive parameters (m_{10}, g_7) were related to the unknown component Y. 6 parameters were related to the rates of *TOC1* mRNA and protein production, degradation and inhibition (n_2, m_5, p_4, p_{15}, g_4, g_6) and 8 parameters were related to the rates of *LHY* mRNA and protein production, degradation and inhibition (p_1, p_3, g_2, g_3, m_1, m_3, n_0, a). The final 9 parameters were related to the production of PRR9, PRR7 and NI (m_{14}, m_{15}, n_7, n_{11}, p_9, g_9, g_{10}, g_{13}, i,), which confirms the importance of the night regulators of *LHY/CCA1* for many characteristics of the clock.

2 Experimental methods

Skeleton photoperiod LUC experiments

Arabidopsis thaliana prr5-11, prr7-3 and *prr7-3/prr5-11* mutants in the Columbia-0 (Col) background were described in (Nakamichi et al, 2005). Plants carried the *CCA1:LUC* (Nakamichi et al, 2004) or *PRR9:LUC* reporter genes. The *PRR9:LUC* line was in Ws background as described (Edwards K. et al., in preparation). Bioluminescence assays of *PRR9:LUC* and *CCA1:LUC* under skeleton photoperiod (SK) entrainment were done as follows. Plants were grown on 0.5 x MS 1.2% agar in 12L:12D under white light (100 µmol m^{-2} /s^{-1}) at 22^{o}C for 6 days. Plants were sprayed with 5 mM luciferin (L8200, Biosynth AG, Staad, Switzerland), 18 hours before being transferred into skeleton light conditions (SK) with “dawn” and “dusk” pulses of light duration of 3 h each (3L:6D:3L:12D), from a combination of blue (15 µmol m^{-2} s^{-1}) and red (5 µmol m^{-2} s^{-1}) LED lights. After 4 days of SK plants were moved into constant light conditions for 3 days under the same B+R LEDs. Bioluminescence was measured for 30 min in every 1h 30 min, starting on the first

day of SK entrainment, using ORCA-II-BT 1024, 16-bit camera cooled to -75°C (Hamamatsu Photonics, Welwyn Garden City , UK). The images were processed using Metamorph 6.0 image analysis software (Molecular Devices Corporation, USA).

The bioluminescence profiles of *CCA1:LUC* and *PRR9:LUC* were normalized to the mean level of bioluminescence for each individual plant (excluding the first 18h of the first day of SK). The data were averaged over at least 9 individual plants of each genotype for *CCA1:LUC*, 18 plants for *PRR9:LUC*. The standard error was plotted on all graphs. Experiments were repeated twice with similar results.

Skeleton photoperiod qPCR experiments

QPCR assays of *CCA1* and *PRR9* were carried out in Col seedlings grown on 0.5 MS, 1.5% agar and 3% sucrose. Following 4 days entrainment under LD cycles of 12:12, seedlings were transferred to the SK photoperiod described above. On the fifth day of the skeleton seedlings were harvested hourly into 500µl RNAlater (Ambion; Austin, Texas, USA). RNA was extracted and reverse transcribed as described previously (Locke et al, 2005). Quantitative PCR was carried out using LightCycler480 SYBR Green1 Master Mix (Roche Diagnostics Ltd, Burgess Hill, UK) in technical triplicate, using the Relative Quantification function of a Light Cycler 480 (Roche Diagnostics Ltd, Burgess Hill, UK) to measure mRNA abundance.. Expression values were normalized against *ACTIN 2* (*ACT2*). Primers for *CCA1* and *ACT2* have previously been described (Edwards et al, 2006; Locke et al, 2005). *PRR9* primers were 5-GATTGGTGGAATTGACAAGC-3 and 5-TCCTCAAATCTTGAGAAGGC-3.

Supplementary Figure 17 below shows the comparison of our qPCR and LUC measurements during SK entrainment of wt plants. It demonstrates a slower decrease of *CCA1:LUC* and *PRR9:LUC* compared to *CCA1* and *PRR9* mRNA, measured by qPCR. This is probably related with the slower degradation rate of *LUC* mRNA and protein compared to rapid degradation of *CCA1* and *PRR9* mRNA and proteins.

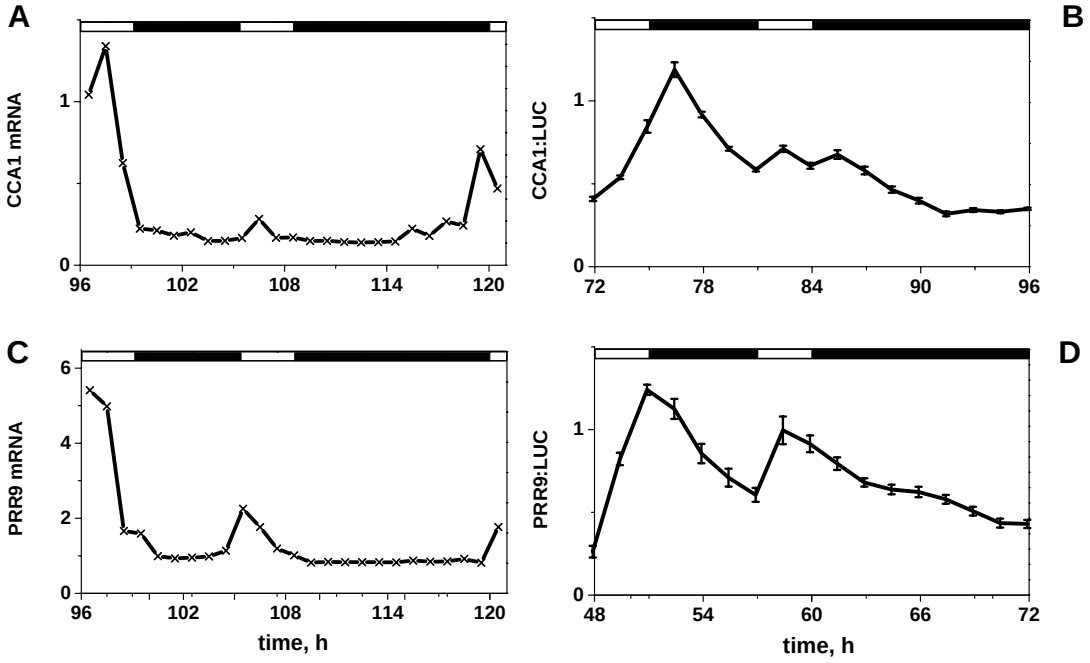

Supplementary Figure 17. Experimental profiles of clock *CCA1* and *PRR9* expression in wt plants during skeleton entrainment (SK). Plants were transferred from 12L:12D to SK entrainment with "dawn" and "dusk" pulses of light, each of 3h duration (3L:6D:3L:12D), at time 0h. A, C: Time course of *CCA1* (A) and *PRR9* (C) expression as determined by qPCR analysis. B, D: Normalized luminescence of *CCA1:LUC* (B) and *PRR9:LUC* (D).

TOC1 and CCA1 mRNA Stability Measurements

The measurements followed standard protocols (Gutierrez et al, 2002; Johnson et al, 2000; Seeley et al, 1992). Briefly, plants of *Arabidopsis thaliana* ecotype Columbia were grown for 6 days at 22°C in 12L:12D cycles on 1.5% Agar plates containing MS and 3% Sucrose. At the end of the last dark period plants were transferred to constant light. 23h after transfer to constant light the plants were removed from the plates and placed in liquid incubation buffer (1 mM PIPES, pH 6.25, 1 mM sodium citrate, 1 mM KCI, and 15 mM Sucrose). After 2h, cordycepin (Sigma-Aldrich Company Ltd, Dorset, UK) was added to a final concentration of 0.6 mM. Samples were removed

from the cultures, blotted dry and placed into RNAlater (Ambion, Austin, Texas, USA) at the times indicated.

The levels of *TOC1* and *CCA1* mRNA were determined by quantitative real-time PCR (as described in Edwards K. et al., in preparation) in *toc1-ox* and *cca1-ox* lines, respectively, in order to avoid confounding effects from dynamic transcriptional regulation of the native transcripts (Supplementary Figures 18A, B). The experiment was repeated twice as shown on Supplementary Figure 18 by different symbols. The *TOC1* mRNA half-life was 139±17 min. The *CCA1* mRNA half-life was 136 min, in agreement with published data (Yakir et al, 2007). Control experiments with the rapidly-degraded *NIA2* (At1g37130) mRNA (Supplementary Figure 18C) showed a half-life of 48 min, which is in good agreement with the published half-life of 49 min (Lidder et al, 2005).

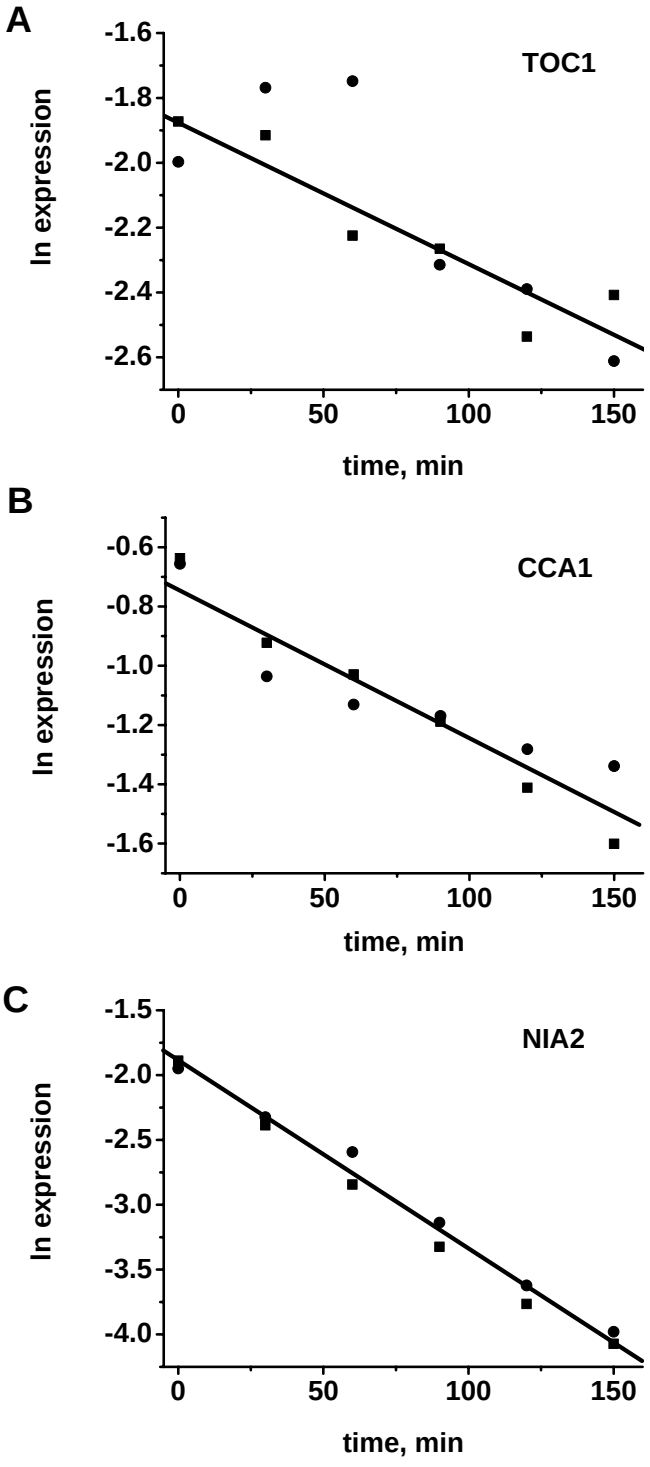

Supplementary Figure 18. Decreasing mRNA abundance after addition of cordycepin to plants in constant light. *TOC1*, *CCA1* and *NIA2* mRNA expression were measured in panels A, B, C, respectively. Experiments were done in a *toc1-ox* line for A and *cca1-ox* line for B, C.

TOC1 expression in lhy/cca1 *under diurnal conditions*

Arabidopsis thaliana lhy/cca1 mutants with the *TOC1:LUC* reporter in the Wassileskija (Ws) background were described in (Hall et al, 2003). Plants were grown on 0.5 x MS 1.2% agar in LD (18 h light/6 h dark) or SD (6 h light/18 h dark) under white light (100 µmol m^{-2} /s^{-1}) at 22°C for 6 days. Bioluminescence was measured under the entrainment conditions under R+B LED's, and normalized (excluding the first day of imaging) as described above in the section *Skeleton photoperiod LUC experiments*. The data was averaged on at least 56 individual plants. The standard error was plotted on all graphs.

Supplementary Figure 19 below shows that the bioluminescence profile of *TOC1:LUC* in the *lhy/cca1* mutant has a much broader peak in the long (18L:6D) days compared to the short (6L:18D) days, which corresponds to the model prediction on Figure 2B of the Results.

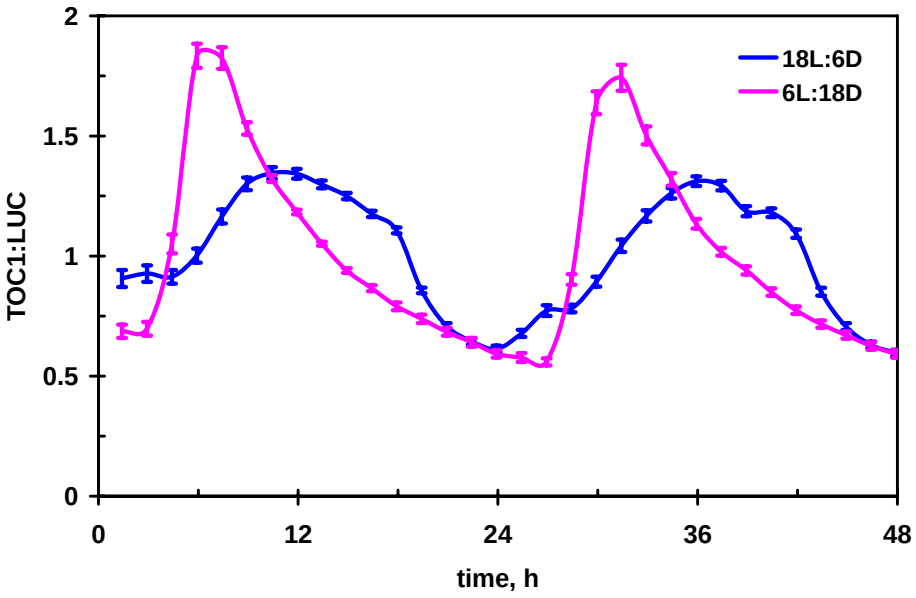

Supplementary Figure 19. Bioluminescence of *TOC1:LUC* in *lhy/cca1* mutant plants under short and long photoperiods.

Acknowledgments

The authors are grateful to Ake Henrik Johansson for creating Supplementary Figure 1 in SBGN format. We are grateful to Edinburgh Parallel Computing Centre (EPCC; http://www.epcc.ed.ac.uk/) for compute time on their BlueGene/L service.

3 References

Akman OE, Locke JC, Tang S, Carre I, Millar AJ, Rand DA (2008) Isoform switching facilitates period control in the Neurospora crassa circadian clock. *Mol Syst Biol* **4:** 164

Baudry A, Ito S, Song YH, Strait AA, Kiba T, Lu S, Henriques R, Pruneda-Paz JL, Chua NH, Tobin EM, Kay SA, Imaizumi T (2010) F-box proteins FKF1 and LKP2 act in concert with ZEITLUPE to control Arabidopsis clock progression. *Plant Cell* **22:** 606-622

Daniel X, Sugano S, Tobin EM (2004) CK2 phosphorylation of CCA1 is necessary for its circadian oscillator function in Arabidopsis. *Proc Natl Acad Sci U S A* **101:** 3292-3297

Edwards KD, Anderson PE, Hall A, Salathia NS, Locke JC, Lynn JR, Straume M, Smith JQ, Millar AJ (2006) FLOWERING LOCUS C mediates natural variation in the high-temperature response of the Arabidopsis circadian clock. *Plant Cell* **18:** 639-650

Farre EM, Harmer SL, Harmon FG, Yanovsky MJ, Kay SA (2005) Overlapping and distinct roles of PRR7 and PRR9 in the Arabidopsis circadian clock. *Curr Biol* **15:** 47-54

Farre EM, Kay SA (2007) PRR7 protein levels are regulated by light and the circadian clock in Arabidopsis. *Plant J* **52:** 548-560

Gutierrez RA, Ewing RM, Cherry JM, Green PJ (2002) Identification of unstable transcripts in Arabidopsis by cDNA microarray analysis: rapid decay is associated with a group of touch- and specific clock-controlled genes. *Proc Natl Acad Sci U S A* **99:** 11513-11518

Hall A, Bastow RM, Davis SJ, Hanano S, McWatters HG, Hibberd V, Doyle MR, Sung S, Halliday KJ, Amasino RM, Millar AJ (2003) The TIME FOR COFFEE gene maintains the amplitude and timing of Arabidopsis circadian clocks. *Plant Cell* **15:** 2719-2729

Hindmarsh AC BP, Grant KE, Lee SL, Serban R, Shumaker DE, Woodward CS (2005) SUNDIALS: Suite of Nonlinear and Differential/Algebraic Equation Solvers. *ACM Transactions on Mathematical Software* **31:** 363-396

Ito S, Nakamichi N, Kiba T, Yamashino T, Mizuno T (2007) Rhythmic and light-inducible appearance of clock-associated pseudo-response regulator protein PRR9 through programmed degradation in the dark in Arabidopsis thaliana. *Plant Cell Physiol* **48:** 1644-1651

Johnson MA, Perez-Amador MA, Lidder P, Green PJ (2000) Mutants of Arabidopsis defective in a sequence-specific mRNA degradation pathway. *Proc Natl Acad Sci U S A* **97:** 13991-13996

Kiba T, Henriques R, Sakakibara H, Chua NH (2007) Targeted degradation of PSEUDO-RESPONSE REGULATOR5 by an SCFZTL complex regulates clock function and photomorphogenesis in Arabidopsis thaliana. *Plant Cell* **19:** 2516-2530

Kim JY, Song HR, Taylor BL, Carre IA (2003) Light-regulated translation mediates gated induction of the Arabidopsis clock protein LHY. *Embo J* **22:** 935-944

Kim WY, Fujiwara S, Suh SS, Kim J, Kim Y, Han L, David K, Putterill J, Nam HG, Somers DE (2007) ZEITLUPE is a circadian photoreceptor stabilized by GIGANTEA in blue light. *Nature* **449:** 356-360

Le Novere N, Bornstein B, Broicher A, Courtot M, Donizelli M, Dharuri H, Li L, Sauro H, Schilstra M, Shapiro B, Snoep JL, Hucka M (2006) BioModels Database: a free, centralized database of curated, published, quantitative kinetic models of biochemical and cellular systems. *Nucleic Acids Res* **34:** D689-691

Lidder P, Gutierrez RA, Salome PA, McClung CR, Green PJ (2005) Circadian control of messenger RNA stability. Association with a sequence-specific messenger RNA decay pathway. *Plant Physiol* **138:** 2374-2385

Locke JC, Kozma-Bognar L, Gould PD, Feher B, Kevei E, Nagy F, Turner MS, Hall A, Millar AJ (2006) Experimental validation of a predicted feedback loop in the multi-oscillator clock of Arabidopsis thaliana. *Mol Syst Biol* **2:** 59

Locke JC, Southern MM, Kozma-Bognar L, Hibberd V, Brown PE, Turner MS, Millar AJ (2005) Extension of a genetic network model by iterative experimentation and mathematical analysis. *Mol Syst Biol* **1:** 2005 0013

Makino S, Matsushika A, Kojima M, Yamashino T, Mizuno T (2002) The APRR1/TOC1 quintet implicated in circadian rhythms of Arabidopsis thaliana: I. Characterization with APRR1-overexpressing plants. *Plant Cell Physiol* **43:** 58-69

Mas P, Alabadi D, Yanovsky MJ, Oyama T, Kay SA (2003a) Dual role of TOC1 in the control of circadian and photomorphogenic responses in Arabidopsis. *Plant Cell* **15:** 223-236

Mas P, Kim WY, Somers DE, Kay SA (2003b) Targeted degradation of TOC1 by ZTL modulates circadian function in Arabidopsis thaliana. *Nature* **426:** 567-570

Matsushika A, Imamura A, Yamashino T, Mizuno T (2002) Aberrant expression of the light-inducible and circadian-regulated APRR9 gene belonging to the circadian-

associated APRR1/TOC1 quintet results in the phenotype of early flowering in Arabidopsis thaliana. *Plant Cell Physiol* **43:** 833-843

Millar AJ, Straume M, Chory J, Chua NH, Kay SA (1995) The regulation of circadian period by phototransduction pathways in Arabidopsis. *Science* **267:** 1163-1166

Nakamichi N, Ito S, Oyama T, Yamashino T, Kondo T, Mizuno T (2004) Characterization of plant circadian rhythms by employing Arabidopsis cultured cells with bioluminescence reporters. *Plant Cell Physiol* **45:** 57-67

Nakamichi N, Kiba T, Henriques R, Mizuno T, Chua NH, Sakakibara H (2010) PSEUDO-RESPONSE REGULATORS 9, 7, and 5 are transcriptional repressors in the Arabidopsis circadian clock. *Plant Cell* **22:** 594-605

Nakamichi N, Kita M, Ito S, Yamashino T, Mizuno T (2005) PSEUDO-RESPONSE REGULATORS, PRR9, PRR7 and PRR5, together play essential roles close to the circadian clock of Arabidopsis thaliana. *Plant Cell Physiol* **46:** 686-698

Nakamichi N, Matsushika A, Yamashino T, Mizuno T (2003) Cell autonomous circadian waves of the APRR1/TOC1 quintet in an established cell line of Arabidopsis thaliana. *Plant Cell Physiol* **44:** 360-365

Pruneda-Paz JL, Breton G, Para A, Kay SA (2009) A functional genomics approach reveals CHE as a component of the Arabidopsis circadian clock. *Science* **323:** 1481-1485

Roden LC, Song HR, Jackson S, Morris K, Carre IA (2002) Floral responses to photoperiod are correlated with the timing of rhythmic expression relative to dawn and dusk in Arabidopsis. *Proc Natl Acad Sci U S A* **99:** 13313-13318

Seeley KA, Byrne DH, Colbert JT (1992) Red Light-Independent Instability of Oat Phytochrome mRNA in Vivo. *Plant Cell* **4:** 29-38

Southern MM (2005) Mutants in the arabidopsis circadian clock. PhD Thesis, Department of Molecular Cell Biology, University of Warwick, Warwick

Strayer C, Oyama T, Schultz TF, Raman R, Somers DE, Mas P, Panda S, Kreps JA, Kay SA (2000) Cloning of the Arabidopsis clock gene TOC1, an autoregulatory response regulator homolog. *Science* **289:** 768-771

Yakir E, Hilman D, Hassidim M, Green RM (2007) CIRCADIAN CLOCK ASSOCIATED1 transcript stability and the entrainment of the circadian clock in Arabidopsis. *Plant Physiol* **145:** 925-932